

## Application of Inductively Coupled Plasma Quadrupole Mass Spectrometry for the Determination of Monazite Ages by Lead Isotope Ratios

José Marcus Godoy,<sup>\*,a,b</sup> Maria Luiza D. P. Godoy<sup>a</sup> and Cláudia C. Aronne<sup>b</sup>

<sup>a</sup>Instituto de Radioproteção e Dosimetria (IRD), CP 37750, Barra da Tijuca, 22642-970 Rio de Janeiro-RJ, Brazil

<sup>b</sup>Departamento de Química, Pontifícia Universidade Católica do Rio de Janeiro, Rua Marquês de São Vicente 225, 22453-900 Rio de Janeiro-RJ, Brazil

A fim de avaliar a aplicabilidade da espectrometria de massa com plasma indutivamente acoplado à determinação de idades Pb/Pb, U/Pb e Th/Pb de monazitas, estudos foram realizados, inicialmente, em padrões isotópicos de referência para chumbo (NIST SRM 981 e 982). Posteriormente, a metodologia otimizada foi aplicada a areias monazíticas de três diferentes locais, Pão de Açúcar (Rio de Janeiro), Buena (Estado do Rio de Janeiro) e Praia Negra (Guarapari, Estado do Espírito Santo); as idades médias obtidas, (581 ± 21)Ma, (552 ± 32)Ma e (535 ± 3)Ma, respectivamente, estão de acordo com os valores da literatura para amostras de zircão e de monazita dos mesmos locais. Idades Th/Pb com mono-grãos foram também determinadas para a amostra de monazita da Praia Negra, nove grãos foram analisados e o valor médio, (530 ± 26)Ma, está no acordo com o valor obtido com alíquotas maiores. Finalmente, o método foi aplicado a uma amostra de torianita do Estado de Amapá e as idades obtidas Th-Pb, U-Pb e Pb-Pb foram de (2,15 ± 0,05)Ga, (2,03 ± 0,01)Ga e (2,044 ± 0,006)Ga, respectivamente, com um valor médio de (2,08 ± 0,07)Ga, coerente com a idade de (2,08 ± 0,02)Ga do complexo de Bacuri, Amapá, relatada na literatura.

In order to evaluate the applicability of inductively coupled plasma quadrupole mass spectrometry to the determination of Pb/Pb, U/Pb and Th/Pb ages of monazite, studies were carried out initially applying lead atom ratio reference standards (NIST SRM 981 and 982). Further, the optimized methodology was applied to monazite sands from three different sites, Sugar Loaf Hill (Rio de Janeiro city), Buena (Rio de Janeiro state) and Black Sands Beach (Guarapari, Espírito Santo state); the obtained mean ages, (581 ± 21)Myers, (552 ± 32)Myers and (535 ± 3)Myers, respectively, are in agreement with the literature values for zircon and monazite samples from the same sites. Single grain Th/Pb ages were also determined for the monazite sample from Black Sands beach, nine grains were analyzed and the mean value, (530 ± 26)Myers, is in agreement with the value obtained with bulk samples. Finally, the method was applied to a thorianite sample from Amapá state and the observed Th-Pb, U-Pb and Pb-Pb ages obtained were (2.15 ± 0.05)Gyears, (2.03 ± 0.01)Gyears and (2.044 ± 0.006)Gyears respectively, with a mean value of (2.08 ± 0.07)Gyears. This value is coherent with the (2.08 ± 0.02)Gyears age of the Bacuri complex, Amapá, reported in the literature.

**Keywords:** inductively coupled plasma mass spectrometry (ICP-MS), lead dating, monazite

### Introduction

Considering the four stable isotopes of lead, only <sup>204</sup>Pb is non-radiogenic. Since the other three, <sup>206</sup>Pb, <sup>207</sup>Pb and <sup>208</sup>Pb, are end-members of the <sup>232</sup>Th (<sup>208</sup>Pb), <sup>235</sup>U (<sup>207</sup>Pb) and <sup>238</sup>U (<sup>206</sup>Pb) radioactive decay chains, different minerals show different isotopic compositions according

to their age and the initial Th and U content of the source rock.<sup>1</sup> Although less resistant than zircon, monazite offers the advantage of generally higher U and Th content and often behaves as a closed-system for U and Pb.<sup>2</sup>

For the purpose of lead dating, thermal ionization mass spectrometry (TIMS) using a magnetic sector mass analyzer has been the conventional method for high precision isotopic analysis with relative standard deviations (RSD) lower than 0.01% when applied to reference materials, NIST-SRM-

\*e-mail: jmgodoy@rdc.puc-rio.br

981<sup>3-5</sup> or BCR-SRM-278 (Mussel Tissue), NIST-SRM-1577A (Bovine Liver) and BCR-SRM-422 (Cod Muscle).<sup>6</sup> However, the precision values obtained for real samples are in the range of 0.1-0.3%.<sup>7-9</sup> Moreover, the relatively high cost of TIMS instrumentation and the extensive chemical pre-treatment required have imposed limitations on the routine use of TIMS techniques in geochemical exploration applications.<sup>5,10,11</sup>

Although the quadrupole inductively coupled plasma mass spectrometry (ICP-MS) shows inferior precision in comparison with TIMS, it has some important advantages, such as (i) simple sample pre-treatment, (ii) high sample throughput and simple sample introduction and (iii) widespread availability.<sup>12</sup>

Quadrupole based ICP-MS instruments have been used in many studies to measure Pb atom ratios. The precisions measured in reference materials are typically 0.1- 0.3% RSD,<sup>13-16</sup> whereas for real samples, a precision in the range of 0.2-0.5% RSD is usually obtained.<sup>8,9,17,18</sup> Despite the fact that quadrupole based instruments may offer a precision 100 times worse than that obtained with TIMS for reference materials, when applied to real samples this difference is reduced to less than one order of magnitude.<sup>6-9,19</sup> Several factors may be responsible for this variability, but the most important factors affecting the precision are those regarding the sample variance, including sample and sample preparation uncertainties, sample matrix effects and chemical steps associated with the method other than with the instrumental technique itself.<sup>7-9</sup>

In the present work, the application of quadrupole ICP-MS for the determination of lead atom ratios has been evaluated by aiming at its application for dating of monazites, using the <sup>206</sup>Pb/<sup>238</sup>U, <sup>208</sup>Pb/<sup>232</sup>Th, <sup>207</sup>Pb/<sup>206</sup>Pb and U-Th-total Pb methods.

## Experimental

### Instrumentation

A Perkin-Elmer SCIEX ELAN 6000 ICP-MS equipped with the original cross flow nebulizer was used for the Pb isotopic measurement. A peristaltic pump performed the solution aspiration. The ICP-MS instrumental operating conditions are summarized in Table 1.

### Reagents and standard solutions

All reagents used were of analytical-reagent grade or higher purity and de-ionized water was further purified using a Millipore Milli-Q water purification system. Certified lead atom ratio standard materials (SRM 981

**Table 1.** Perkin-Elmer SCIEX ELAN 6000 ICP-MS operation conditions

Operation conditions	
RF Power / (W)	1050
Plasma gas flow rate / (L min <sup>-1</sup> )	17
Auxiliary gas flow rate / (L min <sup>-1</sup> )	1.2
Nebulizer gas flow rate / (L min <sup>-1</sup> )	0.9
Sample uptake rate / (mL min <sup>-1</sup> )	1.0
Scan mode	Peak hopping
Lens scanning	Enabled
Detector mode	Dual – Pulse and Analog
Replicates	6
Sweeps / replicate	200
Dwell time / (ms)	<sup>202</sup> Hg = 300
	<sup>204</sup> Pb = 300
	<sup>206</sup> Pb = 20
	<sup>207</sup> Pb = 20
	<sup>208</sup> Pb = 10

and (SRM 982) were purchased from the National Institute of Standards and Technology (NIST, USA).

### Monazite samples

#### Buena monazite sample

A pure monazite concentrate sample from Buena (São Francisco de Assis county), in the north of the Rio de Janeiro State (Brazil), was obtained from INB (Indústrias Nucleares Brasileiras).

#### Sugar Loaf Hill and Black Sand beach samples

In both locations (Urca beach, Rio de Janeiro/RJ) and Black Sand Beach (BSB) (Guarapari, ES), the area with the highest radioactivity was localized with a cintilometer and approximately 5 kg sand samples were taken. The monazite fraction was separated as described by Barling *et al.*<sup>20</sup>

### Sample dissolution and analysis

For each sample, a bulk sample was prepared by crushing, by hand, several monazite grains using an agate mortar. Three 25 mg aliquots of each sample, equivalent to 150 grains, were weighed, transferred to a 10 mL platinum crucible, to which 500 µL of phosphoric acid was added and then was heated to red-hot for a few minutes by applying a Meker burner. A clear solution was observed and diluted to 10 mL with 7.2 mol L<sup>-1</sup> nitric acid. One milliliter was removed and diluted to 50 mL with 2% (v/v) nitric acid. All determinations were standardized against a reagent blank.

Using this solution, lead, uranium and thorium content were determined by ICP-OES and ICP-MS, respectively, using thallium as internal standard. Each aliquot is analyzed three times and the method standard deviation is 1% for lead and uranium and 2% for thorium.

Prior to the lead isotopic ratio determinations, the mass bias correction factor for  $^{204}\text{Pb}$ ,  $^{207}\text{Pb}$  and  $^{208}\text{Pb}$  related to  $^{206}\text{Pb}$  were determined using the NIST-SRM-981 ( $10\ \mu\text{g L}^{-1}$ ). The obtained values were verified using the NIST-SRM-982 ( $10\ \mu\text{g L}^{-1}$ ) as a sample. These factors were verified at the end of each sample batch, analyzing the NIST-SRM-981 solution as a sample. One percent relative bias was specified as a limit for recalibration and sample reanalysis and during the present work no reanalysis was necessary.

### Age calculation

In order to calculate the  $^{206}\text{Pb}/^{238}\text{U}$ ,  $^{208}\text{Pb}/^{232}\text{Th}$  and  $^{207}\text{Pb}/^{206}\text{Pb}$  ages the following methodology was adopted. Based on the  $^{204}\text{Pb}/^{206}\text{Pb}$ ,  $^{207}\text{Pb}/^{206}\text{Pb}$  and  $^{208}\text{Pb}/^{206}\text{Pb}$  atom ratios, the  $^{204}\text{Pb}$ ,  $^{206}\text{Pb}$ ,  $^{207}\text{Pb}$  and  $^{208}\text{Pb}$  atom percent was calculated. The radiogenic  $^{206}\text{Pb}$ ,  $^{207}\text{Pb}$  and  $^{208}\text{Pb}$  atom percentages were calculated according to equations 1-3, where the  $(^{206}\text{Pb}/^{204}\text{Pb})_{\text{nat}}$ ,  $(^{207}\text{Pb}/^{204}\text{Pb})_{\text{nat}}$ ,  $(^{208}\text{Pb}/^{204}\text{Pb})_{\text{nat}}$  ratios were obtained based on the NIST-SRM-981 lead isotopic composition.

$$(^{206}\text{Pb})_{\text{rad}} = (^{206}\text{Pb})_{\text{exp}} - (^{206}\text{Pb}/^{204}\text{Pb})_{\text{nat}} \times (^{204}\text{Pb})_{\text{exp}} = (^{206}\text{Pb})_{\text{exp}} - 16.9374 (^{204}\text{Pb})_{\text{exp}} \quad (1)$$

$$(^{207}\text{Pb})_{\text{rad}} = (^{207}\text{Pb})_{\text{exp}} - (^{207}\text{Pb}/^{204}\text{Pb})_{\text{nat}} \times (^{204}\text{Pb})_{\text{exp}} = (^{207}\text{Pb})_{\text{exp}} - 15.4916 (^{204}\text{Pb})_{\text{exp}} \quad (2)$$

$$(^{208}\text{Pb})_{\text{rad}} = (^{208}\text{Pb})_{\text{exp}} - (^{208}\text{Pb}/^{204}\text{Pb})_{\text{nat}} \times (^{204}\text{Pb})_{\text{exp}} = (^{208}\text{Pb})_{\text{exp}} - 36.7219 (^{204}\text{Pb})_{\text{exp}} \quad (3)$$

Based on these results, the  $^{206}\text{Pb}/^{238}\text{U}$ ,  $^{208}\text{Pb}/^{232}\text{Th}$  and  $^{207}\text{Pb}/^{206}\text{Pb}$  ages were calculated according to equations 4-6:

$$(^{206}\text{Pb})_{\text{rad}} = ^{238}\text{U} (e^{-\lambda_{238}t} - 1) \quad (4)$$

$$(^{208}\text{Pb})_{\text{rad}} = ^{232}\text{Th} (e^{-\lambda_{232}t} - 1) \quad (5)$$

$$(^{207}\text{Pb})_{\text{rad}} / (^{206}\text{Pb})_{\text{rad}} = ^{238}\text{U} / ^{235}\text{U} [(e^{-\lambda_{238}t} - 1) / (e^{-\lambda_{235}t} - 1)] = 137.88 [(e^{-\lambda_{238}t} - 1) / (e^{-\lambda_{235}t} - 1)] \quad (6)$$

where:

$$\lambda_{238} = ^{238}\text{U} \text{ decay constant} = 1.55125 \times 10^{-10} \text{ year}^{-1}$$

$$\lambda_{235} = ^{235}\text{U} \text{ decay constant} = 9.8485 \times 10^{-10} \text{ year}^{-1}$$

$$\lambda_{232} = ^{232}\text{Th} \text{ decay constant} = 0.49475 \times 10^{-10} \text{ year}^{-1}$$

In equations 1-3  $(^{\text{xxx}}\text{Pb})_{\text{rad}}$  are expressed as mass concentration, while in equations 4-6  $(^{206}\text{Pb})_{\text{rad}}$ ,  $(^{207}\text{Pb})_{\text{rad}}$ ,  $(^{208}\text{Pb})_{\text{rad}}$ , as well as  $^{238}\text{U}$  and  $^{232}\text{Th}$ , are expressed as number of moles per sample mass.

Additionally to the  $^{206}\text{Pb}/^{238}\text{U}$ ,  $^{208}\text{Pb}/^{232}\text{Th}$  and  $^{207}\text{Pb}/^{206}\text{Pb}$  ages, it was tested the U-Th-total Pb method, applying the equation described by Rhede *et al.*<sup>21</sup> and supposing that all lead is radiogenic.

$$\text{Pb}_{\text{total}} = 0.8929 \text{ Th} (e^{-\lambda_{232}t} - 1) + \text{U} [0.8643 (e^{-\lambda_{238}t} - 1) + 0.00639 (e^{-\lambda_{235}t} - 1)] \quad (7)$$

## Results and Discussion

### Atom ratio precision and accuracy

Many factors directly control the signal acquisition process on the ELAN 6000 ICP-MS. Some are automatically optimized; others can be manually controlled, among them, the dwell time, the number of sweeps/replicate and the number of replicates/analysis. These three parameters were selected in this study in order to determine the best operation condition. Initially, the default operation conditions were applied and a high RSD was obtained. Considering the different atom ratios involved, better results were achieved by applying different dwell times for each isotope, higher for  $^{204}\text{Pb}$ , the least abundant, and lower for  $^{208}\text{Pb}$ , the most abundant, according Platzner *et al.*<sup>14</sup>

Based on the ELAN 6000 operation manual,<sup>22</sup> the dwell time for each isotope was calculated in order to obtain  $10^6$  counts/replicate, using 200 sweeps/replicate. Also based on that, ten replicates/analysis was chosen. As the sample volume required and the time expended for each sample were too high, the same calculation was performed for 500.000 counts and 6 replicates/analysis.  $^{202}\text{Hg}$  was also included because of a potential isobaric interference of  $^{204}\text{Hg}$ , a dwell time equal to that of  $^{204}\text{Pb}$  was chosen (Table 1).

Based on the NIST SRM 981, 1.5, 7.5, 15, 30 and 45  $\mu\text{g Pb L}^{-1}$  solutions were prepared. The  $^{204}\text{Pb}$ ,  $^{206}\text{Pb}$ ,  $^{207}\text{Pb}$  and  $^{208}\text{Pb}$  values obtained using the 10  $\mu\text{g Pb L}^{-1}$  standard solution were used to calculate the mass fractionation correction factor for  $^{204}\text{Pb}$ ,  $^{207}\text{Pb}$  and  $^{208}\text{Pb}$  related to  $^{206}\text{Pb}$ . Using these factors,  $^{204}\text{Pb}/^{206}\text{Pb}$ ,  $^{207}\text{Pb}/^{206}\text{Pb}$  and  $^{208}\text{Pb}/^{206}\text{Pb}$  atom ratios were calculated and results are shown in Figure 1. For lead concentrations higher than 20  $\mu\text{g L}^{-1}$ ,  $^{208}\text{Pb}/^{206}\text{Pb}$  ratios lower than the certified value were obtained due to dead time effects on the  $^{208}\text{Pb}$  determination. This concentration can be taken as an upper limit of lead in the sample solution.

According to Platzner *et al.*,<sup>14</sup> it is possible to reduce the relative standard deviation, in isotope composition determinations using a quadrupole ICP-MS with consecutive measurements. This procedure of multiple determinations was performed employing a solution of 10  $\mu\text{g L}^{-1}$  of SRM 981 to nine sequential determinations. The previous procedure was repeated using a 10  $\mu\text{g L}^{-1}$  SRM 982 solution. The results are listed in Table 2 and show that precision better than 0.25% (95% confidence limits) as well as accuracy in the range of 0.1 to 2% can be achieved. In general, for  $^{204}\text{Pb}/^{206}\text{Pb}$ ,  $^{207}\text{Pb}/^{206}\text{Pb}$  and  $^{208}\text{Pb}/^{206}\text{Pb}$  atom ratios, the relative bias increases with the distance to an atom ratio equal to one.

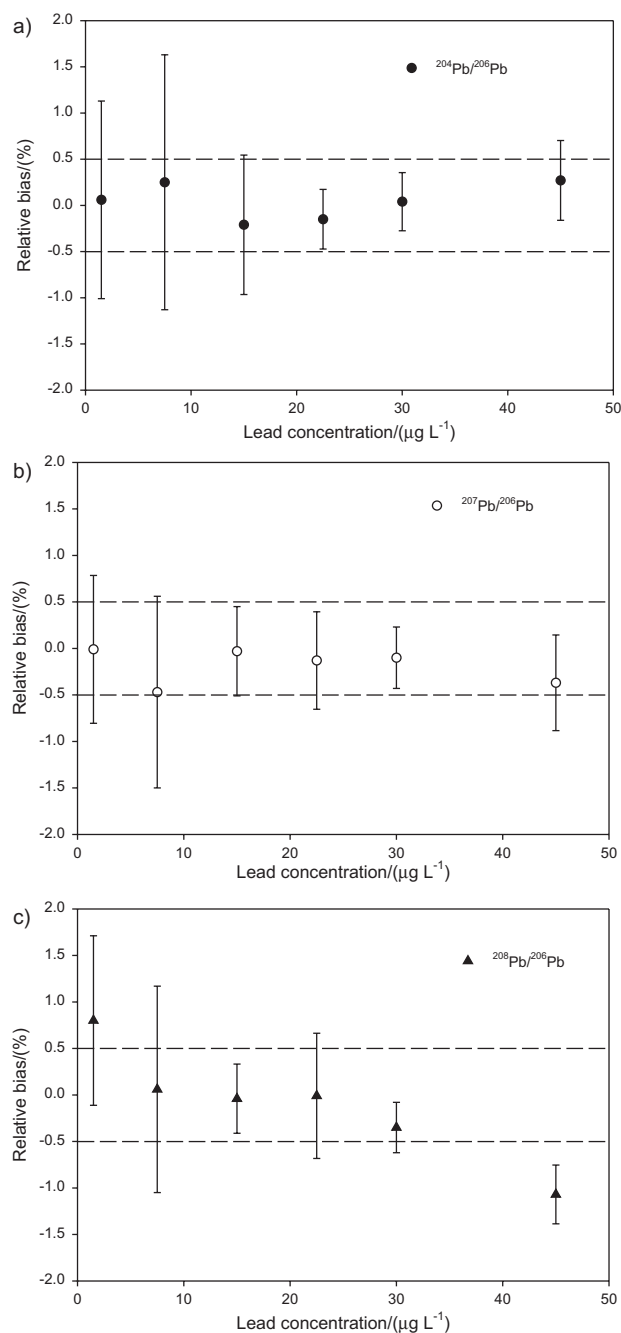


**Figure 1.** Influence of the lead concentration on the  $^{204}\text{Pb}/^{206}\text{Pb}$  (a),  $^{207}\text{Pb}/^{206}\text{Pb}$  (b) and  $^{208}\text{Pb}/^{206}\text{Pb}$  (c) atom ratio accuracy.

### Bulk samples

The lead, uranium and thorium contents of the three analyzed monazite samples and the observed lead atom ratio are shown in Table 3. For each individual aliquot, the monazite ages were calculated applying the  $^{206}\text{Pb}/^{238}\text{U}$ ,  $^{208}\text{Pb}/^{232}\text{Th}$ ,  $^{207}\text{Pb}/^{206}\text{Pb}$  and U-Th-total Pb methods and the obtained values are shown in Table 4. The agreement between the results of the  $^{206}\text{Pb}/^{238}\text{U}$  and  $^{208}\text{Pb}/^{232}\text{Th}$  dating methods shows the proposed procedure reliability. The association of a higher thorium content with a lower uranium concentration leads to a low  $^{207}\text{Pb}$  signal and to a large standard deviation related to the  $^{207}\text{Pb}/^{206}\text{Pb}$  age. The calculated U-Th-total Pb ages were in the range of the  $^{206}\text{Pb}/^{238}\text{U}$ ,  $^{208}\text{Pb}/^{232}\text{Th}$  and  $^{207}\text{Pb}/^{206}\text{Pb}$  ages showing that, at least, for monazite samples this relatively simple method can provide results that could be used as a starting point for further studies applying more accurate methods based on multi-collector mass spectrometers.

The obtained Sugar Loaf Hill  $^{238}\text{U}/^{206}\text{Pb}$  age is coherent with the 560 Myears value published by Silva and Ramos.<sup>23</sup> Moreover, the obtained ages are in agreement with Brasiliano orogeny.<sup>24-26</sup>

The overall compositional variations among various monazite types are governed by substitution of REE by Th and U.<sup>27,28</sup> Therefore, since the observed uranium

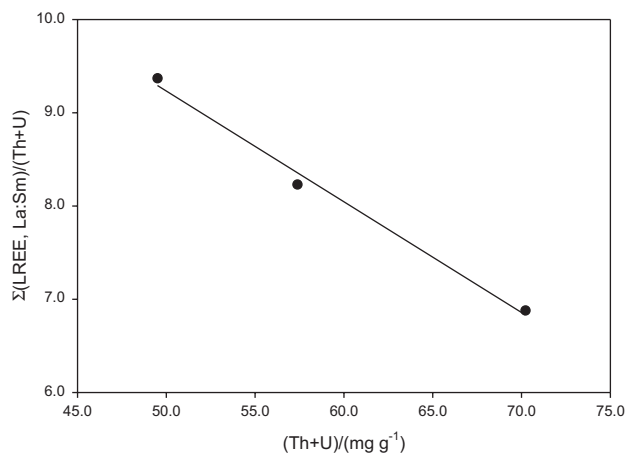


**Figure 2.** Light rare-earth elements (La:Sm) content relationship with the actinide (Th+U) concentration.

**Table 2.** Results for the analysis of lead atom ratio standard reference materials, errors are based on 95% confidence limits

	SRM 981			SRM 982		
	$^{204}\text{Pb}/^{206}\text{Pb}$	$^{207}\text{Pb}/^{206}\text{Pb}$	$^{208}\text{Pb}/^{206}\text{Pb}$	$^{204}\text{Pb}/^{206}\text{Pb}$	$^{207}\text{Pb}/^{206}\text{Pb}$	$^{208}\text{Pb}/^{206}\text{Pb}$
Reference value	0.059042	0.91464	2.1681	0.027219	0.46707	1.00016
Relative error / (%)	0.063	0.036	0.037	0.10	0.043	0.030
Mean value (n=9)	0.058761	0.91353	2.1886	0.027782	0.46550	0.997151
Relative error of the mean / (%)	0.16	0.12	0.22	0.26	0.08	0.12
Relative bias / (%)	$-(0.48 \pm 0.17)$	$-(0.12 \pm 0.13)$	$(0.95 \pm 0.23)$	$(2.07 \pm 0.28)$	$-(0.34 \pm 0.10)$	$-(0.30 \pm 0.12)$

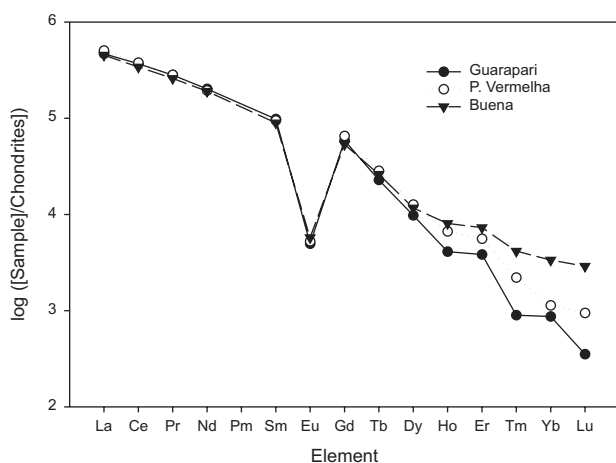
**Table 3.** Observed lead, uranium and thorium contents (in g kg<sup>-1</sup>) and lead atom ratios of the analyzed monazite samples (errors are based on 95% confidence limits)

Sample	Pb	U	Th	<sup>204</sup> Pb/ <sup>206</sup> Pb	<sup>207</sup> Pb/ <sup>206</sup> Pb	<sup>208</sup> Pb/ <sup>206</sup> Pb
Buena	1.24	1.73	46.0	0	0.04814 (2.3%)	8.3803 (0.4%)
	1.24	1.72	45.1	0.00267 (3.6%)	0.09803 (0.5%)	7.9015 (0.2%)
	1.20	1.72	44.5	0.00229 (6.6%)	0.09308 (2.1%)	7.9950 (0.2%)
Sugar Loaf	1.58	1.98	51.2	0.00381 (0.8%)	0.11426 (0.5%)	8.3481 (0.2%)
	1.32	1.68	43.6	0.00460 (6.2%)	0.12718 (3.3%)	8.2653 (0.7%)
Guarapari	1.57	1.24	61.9	0.00041 (4.2%)	0.06221 (0.8%)	15.6519 (0.2%)
	1.47	1.10	55.6	0.00064 (5.8%)	0.06503 (0.5%)	15.7717 (0.2%)
	1.51	1.26	59.3	0.00082 (0.2%)	0.07505 (0.7%)	15.1495 (0.2%)

**Table 4.** Obtained monazite ages, values in Myears (± 95% confidence level)

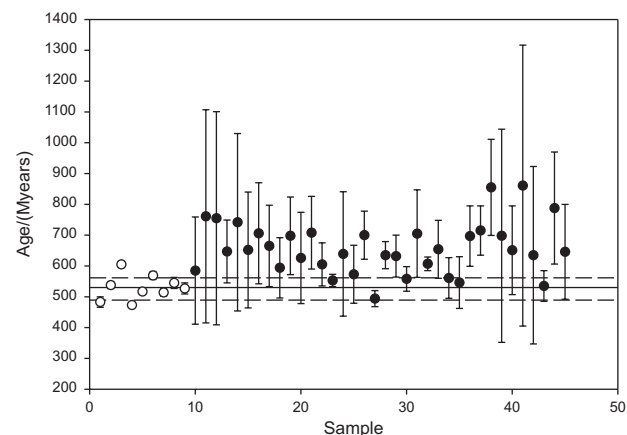
Sample	U/Pb	Th/Pb	Pb/Pb	U-Th-total Pb	Mean Age
Buena	542	531	NC	535	548 (±28)
	543	528	580	545	
	529	522	600	535	
Mean value	538 (±1.6%)	527 (±1.0%)	590	538 (1.3%)	
Sugar Loaf	562	594	570	610	585 (±22)
	549	578	630	600	
	556	586	600	605	
Mean value	556	586	600	605	
Guarapari	537	527	465	533	536 (±4)
	558	549	445	553	
	520	527	550	533	
Mean value	539 (±4.1%)	534 (±2.4%)	532 (±12%)	539 (2.6%)	

and thorium contents were different (Table 3), an additional aliquot of each monazite sample, was taken and uranium, thorium and the rare earth elements (REE) were determined in order to verify if this substitution has occurred. Figure 3 shows that this substitution effectively occurs with an inverse correlation between  $\Sigma(\text{LREE: La-Sm})$  and  $(\text{Th}+\text{U})$ . The chondrite-normalized REE content is shown in Figure 4. All monazite samples have patterns with negative europium anomaly and with similar light REE (LREE) composition. The

**Figure 3.** Rare-earth elements concentration, normalized to the Chondrites, in the studied monazite samples. Chondrite values are taken from Anders and Grevesse (reference 33).

heavy REE are divergent, the largest difference being found for the heaviest elements. Mohanty *et al.*,<sup>27</sup> analyzing monazite sand grain from the Chhatrapur beach placer deposits, have also observed a uniform LREE enrichment with a prominent Eu anomaly, which has been attributed to the preferential incorporation of the LREE during the melting.

The method was also tested on older samples. A thorianite sample from Amapá was obtained from the Brazilian Nuclear Energy Commission. Three 10 mg

**Figure 4.** Black Sand beach monazites: single grain Th/Pb ages obtained in the present work (open dots) in comparison with those reported by Machado and Gauthier (closed dots reference 2), each errors bar represents two standard deviations. The black and the two red reference lines are the mean value and the 95% uncertainties calculated based on the open dot values.

aliquots were taken, and after total dissolution with  $\text{HNO}_3$ -HF- $\text{HClO}_4$ , they were analyzed in the same way as the monazite samples. The obtained mean (95% confidence level)  $^{206}\text{Pb}/^{238}\text{U}$ ,  $^{208}\text{Pb}/^{232}\text{Th}$  and  $^{207}\text{Pb}/^{206}\text{Pb}$  ages were  $(2.15 \pm 0.05)\text{Gyears}$ ,  $(2.03 \pm 0.01)\text{Gyears}$ ,  $(2.044 \pm 0.006)\text{Gyears}$  respectively, with a mean value of  $(2.08 \pm 0.07)\text{Gyears}$ . This value is coherent with the  $(2.08 \pm 0.02)\text{Gyears}$  age of the Bacuri complex, Amapá, reported by Pimentel *et al.*<sup>29</sup>

#### Single grain analysis

Based on the lead content and on the weight of single monazite grain, around 150-200  $\mu\text{g}$ , it should be possible to date single monazite grains using the  $^{208}\text{Pb}/^{232}\text{Th}$  ratio. In order to test it, nine well formed round monazite grains from Black Sand beach, Guarapari/ES, with masses ranging from 170 to 230  $\mu\text{g}$ , were taken and dissolved in 100  $\mu\text{L}$   $\text{H}_3\text{PO}_4$  as already described. Based on the lead content observed in the BSB monazite (Table 3), the obtained melt was dissolved and diluted with 2% v/v  $\text{HNO}_3$  in order to obtain a total lead concentration of ca. 10  $\mu\text{g L}^{-1}$ . The lead and thorium concentrations on each solution was determined and, based on the obtained results, the lead and thorium content of each grain was calculated. Afterward, the same solution was used for the lead atom ratio determination. Using the lead and thorium content and  $^{208}\text{Pb}$  atom ratio,  $^{208}\text{Pb}/^{232}\text{Th}$  ages were calculated (Table 5) and values between 473 and 605 Myears were observed. Similar results were obtained by Machado and Gauthier<sup>2</sup> working with BSB monazites. Figure 4 presents a comparison of the results obtained in the present work and those related by Machado and Gauthier,<sup>2</sup> applying a LA-ICP-QMS. The main source of uncertainty from using the present methodology was the determination of the lead and thorium contents, typically between 0.5 and 1.0%, for both elements. Therefore, the expanded uncertainty for a single grain monazite Th/Pb age is lower than 2%, which is much lower than the  $^{207}\text{Pb}/^{206}\text{Pb}$  age uncertainty obtained by an equivalent LA-ICP-QMS. The observed mean value working with single grains,  $(530 \pm 26)\text{Myears}$ , and with bulk samples,  $(535 \pm 3)\text{Myears}$ , are statistically indistinguishable.

The work of Machado and Gauthier<sup>2</sup> was chosen since it deals with monazite grains taken from the same places as discussed in the present work. However, it is interesting to compare the  $^{206}\text{Pb}/^{207}\text{Pb}$  age uncertainty achieved by them with those obtained in more recent works also applying LA-ICP-QMS.<sup>29-31</sup> It is possible to observe that great improvement was achieved since the Machado and Gauthier work;<sup>2</sup> notwithstanding,

**Table 5.** Lead and thorium contents and  $^{208}\text{Pb}$  atomic percentage observed in Black sand beach, Guarapari, monazite grains, and calculated Th/Pb ages ( $\pm 95\%$  confidence level)

Sample	Pb / ( $\text{mg g}^{-1}$ )	Th / ( $\text{mg g}^{-1}$ )	$^{208}\text{Pb}$ / atom %	Th / Pb age Myears
1	2.038	50.65	97.1426	483 $\pm$ 17
2	2.58	58.32	95.7408	583 $\pm$ 11
3	2.042	53.08	75.9825	605 $\pm$ 10
4	3.495	88.49	97.4197	473 $\pm$ 5
5	2.847	65.84	97.4512	517 $\pm$ 9
6	2.95	64.03	94.2273	569 $\pm$ 13
7	2.788	64.11	98.5611	514 $\pm$ 12
8	3.069	70.78	92.5643	546 $\pm$ 18
9	3.232	73.14	97.5802	527 $\pm$ 18

relatively high uncertainties have still been obtained with mean values ranging from 5.3% to 20.0%.<sup>29, 31</sup> The same authors reported also  $^{208}\text{Pb}/^{232}\text{Th}$  ages with a mean uncertainty of 2.9% and 10.3%, respectively. On the other hand, in general, 1.5%-2% uncertainties were obtained for  $^{206}\text{Pb}/^{238}\text{U}$  ages despite laser-induced elemental fractionation.<sup>30-32</sup>

## Conclusions

The present study has shown that it is possible to obtain useful monazite dates regarding precision and accuracy applying quadrupole ICP-MS. Moreover, the use of monazite allows the direct determination of lead atom ratios without the need of a chemical separation, even for single grain samples. U-Th-total Pb ages were in the range of the  $^{206}\text{Pb}/^{238}\text{U}$ ,  $^{208}\text{Pb}/^{232}\text{Th}$  and  $^{207}\text{Pb}/^{206}\text{Pb}$  ages showing that, at least, for monazite samples this relatively simple method can provide results that could be used as a starting point for further studies applying more accurate methods based on multi-collector mass spectrometers.

## Acknowledgments

The present work was supported by FINEP (Financiadora de Estudos e Projetos) and CAPES (Coordenação de Aperfeiçoamento de Pessoal de Nível Superior). The authors wish to express their gratitude to Claudio Valeriano (UERJ) and Marcio Pimentel (UnB) for their help during different phases of the present work.

## References

- Jager, E.; Hunziker, J.; *Lectures in Isotope Geology*, Springer Verlag: New York, 1979.

2. Machado, N.; Gauthier, G.; *Geochim. Cosmochim. Acta* **1996**, *60*, 5063.
3. Hoven, H.M.; Gaudette, H.E.; Short, F.T.; *Mar. Environ. Res.* **1999**, *48*, 377.
4. Thirwall, M.F.; *Chem. Geol.* **2000**, *163*, 299.
5. Weiss D.J.; Kober, B.; Dolgoplova, A.; Gallagher, K.; Spiro, B.; Le Roux, G.; Mason, T.F.D.; Kylander, M.; Coles, B.J.; *Int. J. Mass Spectrom.* **2004**, *232*, 205.
6. Encinar, J.R.; Garcia-Alonso, J.I.; Sanz-Medel, A.; Main, S.; Turner, P.J.; *J. Anal. At. Spectrom.* **2001**, *16*, 322.
7. Pomies, C.; Cocheire, A.; Guerrot, C.; Marcoux, E.; Lancelot, J.; *Chem. Geol.* **1998**, *144*, 137.
8. Halicz, L.; Erel, Y.; Veron, A.; *At. Spectrosc.* **1996**, *17*, 186.
9. Weiss, D.; Boyle, E.A.; Chavagnac, V.; Herwegh, M.; Wu, J.; *Spectrochim. Acta, Part B* **2000**, *55*, 363.
10. Townsend, A.T.; Yu, Z.; Mcgoldrick, P.; Hutton, J.A.; *J. Anal. At. Spectrom.* **1998**, *13*, 809.
11. Wannemacker, G.; Vanhaecke, F.; Moens, L.; Mele, A.; Thoen, H.; *J. Anal. At. Spectrom.* **2000**, *15*, 323.
12. Prohaska, T.; Watkins, M.; Latkoczy, C.; Wenzel, W.W.; Stinger, G.; *J. Anal. At. Spectrom.* **2000**, *15*, 365.
13. Heumann, K.G.; Gallus, S.M.; Radlinger, G.; Vogl, J.; *J. Anal. At. Spectrom.* **1998**, *13*, 1001.
14. Platzner, I.T.; Becker, J.S.; Dietze, H-J.; *At. Spectrosc.* **1999**, *20*, 6.
15. Becker, J.S.; Dietze, H-J.; *Fresenius J. Anal. Chem.* **2000**, 368, 23.
16. Begley, I.S.; Sharp, B.L.; *J. Anal. At. Spectrom.* **1997**, *12*, 395.
17. Barbaste, M.; Halicz, L.; Galy, A.; Medina, B.; Emterborg, H.; Adams, F. C.; Lobinski, R.; *Talanta* **2001**, *54*, 307.
18. May, T.W.; Wiedmeyer, R.H.; Brown, L.D.; Casteel, S.W.; *At. Spectrosc.* **1999**, *20*, 199.
19. Kylander, M.E.; Weiss, D.J.; Jeffries, T.; Coles, B.J.; *J. Anal. At. Spectrom.* **2004**, *19*, 1275.
20. Barling, J.; Weis, D.; Demaiffe, D.; *Chem. Geol.* **2000**, *165*, 47.
21. Rhede, D.; Wendt, I.; Förster, H-J; *Chem. Geol.* **1996**, *130*, 247.
22. PERKIN-ELMER, *Inductively Coupled Plasma Mass Spectrometer ELAN 6000, software guide*; PERKIN-ELMER SCIEX Instruments: Canada, 1997.
23. Silva, L.C.; Ramos, A.J.L.A. In *Sítios Geológicos e Paleontológicos do Brasil*; Schobbenhaus, C.; Campos, D.A.; Queiroz, E.T.; Winge, M.; Berbert-Born, M.L.C., eds.; DNPM/CPRM, Comissão Brasileira de Sítios Geológicos e Paleobiológicos (SIGEP): Brasília, 2002, pp. 263-268, available at <http://www.unb.br/ig/sigep/sitio067/sitio067.pdf>.
24. Babinski, M.; van Schmus, W.R.; Chemale, F.; *Chem. Geol.* **1999**, *160*, 175.
25. Söllner, J.; Trouw, R.A.J.; *J. S. Am. Earth Sci.* **1997**, *10*, 21.
26. Leite, J.A.D.; Hartmann, L.A.; Fernandes, L.A.D.; McNaughton, N.J.; Soliani Jr, E.; Koester, E.; Santos, J.O.S.; Vasconcellos, M.A.Z.; *J. S. Am. Earth Sci.* **2000**, *13*, 739.
27. Mohanty, A.K.; Das, S.K.; Vijayan, V.; Sengupta, D.; Saha, S.K.; *Nucl. Instrum. Methods Phys. Res., Sect. B* **2003**, *211*, 145.
28. van Emden, B.; Thornber, M.R.; Grahan, J.; Lincoln, F.J.; *Can. Mineral.* **1997**, *35*, 95.
29. Pimentel, M.M.; Spier, C.A.; Ferreira Filho, C.F.; *Rev. Brasil. Geoc.* **2002**, *32*, 1.
30. Horn, I.; Rudnick, R.L.; McDonough, W.F.; *Chem. Geol.* **2000**, *164*, 281.
31. Jeffries, T.E.; Fernandez-Suarez, J.; Corfu, F.; Alonso, G.G.; *J. Anal. At. Spectrom.* **2003**, *18*, 847.
32. Jackson, S.E.; Pearson, N.J.; Griffin, W.L.; Belousova, E.A.; *Chem. Geol.* **2004**, *211*, 47.
33. Anders, E.; Grevesse, N.; *Geochim. Cosmochim. Acta* **1989**, *53*, 197.

Received: December 11, 2006

Web Release Date: August 6, 2007